analytical chemistry

Article

pubs.acs.org/ac

Analysis of the Acidic Proteome with Negative Electron-Transfer Dissociation Mass Spectrometry

Graeme C. McAlister,[†] Jason D. Russell,[†] Neil G. Rumachik,[†] Alexander S. Hebert,[§] John E. P. Syka,[∥] Lewis Y. Geer,[¶] Michael S. Westphall,[⊥] David J. Pagliarini,[‡] and Joshua J. Coon*[,†,§,⊥]

Departments of [†]Chemistry, [‡]Biochemistry, and [§]Biomolecular Chemistry, University of Wisconsin, Madison, Wisconsin, United States

[⊥]Genome Center of Wisconsin, University of Wisconsin, Madison, Wisconsin, United States

[¶]National Center for Biotechnology Information, National Library of Medicine, National Institutes of Health, Bldg. 38A, 8600 Rockville Pike, Bethesda, Maryland 20894, United States

[∥]Thermo Fisher Scientific, San Jose, California, United States

Supporting Information

ABSTRACT: We describe the first implementation of negative electron-transfer dissociation (NETD) on a hybrid ion trap-orbitrap mass spectrometer and its application to high-throughput sequencing of peptide anions. NETD, coupled with high pH separations, negative electrospray ionization (ESI), and an NETD compatible version of OMSSA, is part of a complete workflow that includes the formation, interrogation, and sequencing of peptide anions. Together these interlocking pieces facilitated the identification of more than 2000 unique peptides from *Saccharomyces cerevisiae* representing the most comprehensive analysis of peptide anions by tandem mass spectrometry to date. The same *S. cerevisiae* samples were interrogated using traditional, positive modes of peptide LC-MS/MS analysis (e.g., acidic LC separations, positive ESI, and collision activated dissociation), and the resulting peptide identifications of the different workflows were compared. Due to a decreased flux of peptide anions and a tendency to produce lowly charged precursors, the NETD-based LC-MS/MS workflow was not as sensitive as the positive mode methods. However, the use of NETD readily permits access to underrepresented acidic portions of the proteome by identifying peptides that tend to have lower pI values. As such, NETD improves sequence coverage, filling out the acidic portions of proteins that are often overlooked by the other methods.

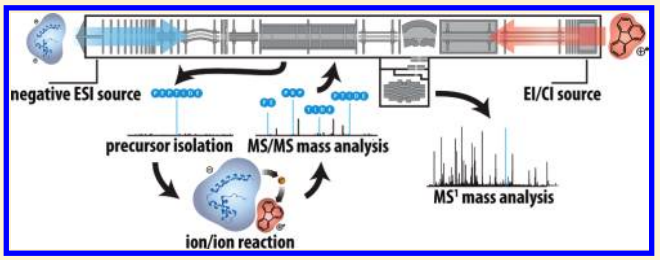

Protein sequence analysis has rapidly evolved over the past decade such that cataloging the presence and abundances of thousands of proteins has become more or less routine, yet limitations still remain. First, identification of all predicted gene products from complex organisms is still out of reach. Second, the amount of coverage for the identified proteins is often very low and may only constitute a few representative peptides. And third, many protein post-translational modifications continue to evade detection by current technology.[1−4] Several factors contribute to these limitations: mass spectrometer duty cycle, dynamic range, and the key but rarely discussed ubiquitous use of positive electrospray ionization (ESI). Achieving good sensitivity in positive ESI during liquid chromatographic separations requires the use of acidic mobile phases (i.e., pH ∼ 3). While peptides and proteins that are highly basic ionize well and are readily detected under these conditions, acidic sequences do not and are subsequently discriminated against. Further, acidic PTMs, like phosphorylation and glycosylation, can bestow similar behavior on otherwise nonacidic sequences. This situation is even further confounding in certain instances where PTMs are acid labile: in histidine phosphorylation, for example, the modification is rapidly lost at pH < 6.[5−9]

Electrospray ionization can be accomplished in the negative mode so that multiply deprotonated peptide ions are generated. Under these conditions, one would optimally employ basic mobile phases during chromatographic separation, which would, in principle, allow access to the portions of the proteome detailed above. The major obstacle, however, in implementing a negative ESI strategy has been tandem mass spectrometry (MS/MS). Subjecting peptide anions to collision-activated dissociation (CAD) produces far less information than the same process does for peptide cations. MS/MS spectra of peptide anions are dominated by neutral losses and internal fragment ions that are difficult to interpret.[10−13] Consequently, these complex spectra make large-scale peptide identification experiments, which rely on simple and predictable fragmentation rules for database correlation, prohibitively difficult.

Received: December 22, 2011
Accepted: February 15, 2012
Published: February 15, 2012

Electron-based fragmentation methods, on the other hand, can effectively generate sequence-informative MS/MS spectra from peptide anions. In this approach, peptide anions are oxidized by either electrons (electron detachment dissociation, EDD) or reagent cations (negative electron-transfer dissociation, NETD) (Figure 1).[14−20] In either case, the newly created radical

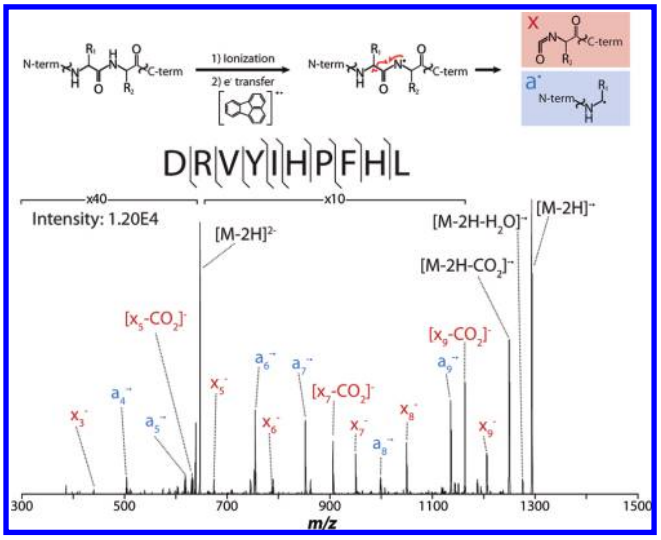

Figure 1. Generalized reaction scheme by which peptide anions are oxidized by fluoranthene radical cations to produce a$^{\bullet}$- and x-type product ions (above).[14,16,19,21] Below is an example NETD MS/MS mass spectrum resulting from the fragmentation of the standard peptide human angiotensin I.

peptide anion undergoes electron rearrangement that often leads to cleavage of the C−C$_{\alpha}$ backbone bond, producing a$^{\bullet}$- and x-type product ions.[14,16,19,21] Electron photodetachment dissociation, a recently developed and intriguing alternative to these electron and cation reagent-based methods of polyanionic peptide fragmentation, uses ultraviolet photons to produce a very similar product ion mixture that primarily consists of a$^{\bullet}$- and x-type fragment ions and has recently been used in the LC-MS/MS analysis of an equimolar mixture of MAPK proteins.[20,22,23] Finally, beyond its application to peptide anion analysis, NETD has also been used to interrogate a range of other analytes (e.g., glycans, RNA, etc.).[24−27]

While both EDD and NETD have existed for several years, neither method has been applied to the analysis of high complexity peptide mixtures; instead, development has been restricted to model peptides and/or simple protein digests.[28,29] Here, we extend NETD capability to a dual cell quadrupole ion trap-orbitrap hybrid mass spectrometer, where high mass accuracy and resolution orbitrap analysis of intact precursor ions allows for sensitive database correlation and false-discovery rate filtering and where fast and sensitive quadrupole ion trap analysis of MS/MS ions allows for rapid interrogation of low-abundance anionic peptide fragment ions. We coupled this modified instrument with a high pH separation strategy that facilitates negative ESI of eluting peptide anions that were generated via enzymatic digestion of *Saccharomyces cerevisiae* (yeast). With this high throughput NETD-based methodology, we demonstrate an ability to investigate previously neglected segments of the proteome.

MATERIALS AND METHODS

All reagents were acquired from Sigma-Aldrich (St. Louis, MO) or Fisher Scientific (Waltham, MA) unless otherwise specified.

Sample Preparation. Protein extraction from wild-type yeast (*S. cerevisiae*) and subsequent digestion with trypsin (Promega, Madison, WI) or GluC (Roche Diagnostics, Indianapolis, IN) was performed as previously described.[3] Exact details can be found in the Supporting Information.

Liquid Chromatography. LC analyses were performed using a nanoACQUITY UltraPerformance LC system (Waters Corp.). Analytical separation columns with integrated ESI emitters were fabricated using 50 μm i.d. × 360 μm o.d. fused silica capillary tubing. ESI emitters were incorporated into analytical columns by pulling a tip with a laser puller (P-2000, Sutter Instrument Company, Novato, CA). Electrospray tip geometry and orifice diameter were optimized by chemical etching with 40% hydrofluoric acid for 2−3 min.[30] Analytical columns were slurry-packed to 15 cm with high pH stable Waters XBridge reversed-phase material (C18, 3.5 μm, 130 Å). Precolumns were fabricated by inserting 75 μm i.d. × 360 μm o.d. capillary into a nanovolume tee (150 μm bore, VICI Valco Instruments CO. INC., Houston, TX) housing a 0.2 μm frit. Precolumns were slurry-packed to 5 cm with the same reversed-phase material while connected to the nanovolume tee. Low pH mobile phase A consisted of 0.2% formic acid, and mobile phase B was 99.8% acetonitrile/0.2% formic acid. Mobile phase A for high pH separations was 5 mM ammonium formate diluted from a stock solution of 250 mM ammonium formate titrated to pH 10 with ammonium hydroxide. Mobile phase B

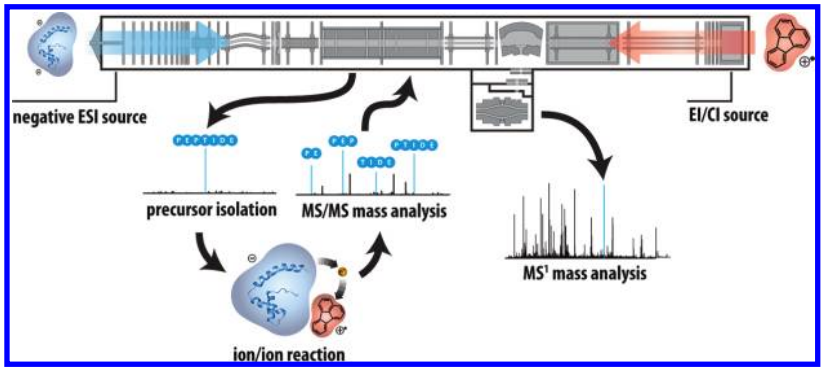

Figure 2. Instrument diagram of the NETD-enabled orbitrap mass spectrometer depicting the sites of anion and cation injection. All MS^1 analyses were performed with the orbitrap. Isolation and activation of peptide anions were performed in the high-pressure quadrupole ion trap, while the resulting MS/MS fragment ion population was analyzed using the low-pressure quadrupole ion trap.

dx.doi.org/10.1021/ac203430u | *Anal. Chem.* 2012, 84, 2875−2882

for high pH separations was 5 mM ammonium formate (diluted from the pH 10 stock) in 85% acetonitrile. Vented configuration trapping for both high and low pH separations was performed at 2% B for 8−10 min at 1−1.25 μL min^{-1}. Gradient elution was performed at 250−300 nL min^{-1}. A typical low pH gradient increased linearly from 2 to 35% B, while high pH gradients increased from 2 to 40% B.

Mass Spectrometry. All data was collected with a modified ETD-enabled hybrid Velos-Orbitrap mass spectrometer (Thermo Fisher Scientific, Bremen, Germany).[31−34] The instrument was modified to facilitate peptide anion fragmentation using NETD ion/ion reactions and to analyze the resulting anionic fragment populations (Figure 2). The instrument modifications involved three principal changes: (1) the chemical ionization (CI) source conditions were adjusted to generate fluoranthene reagent cations, (2) the voltages applied to the ion optics between the CI sources and the dual-cell linear quadrupole ion trap were optimized to transmit reagent cations, and (3) the firmware of the mass spectrometer was rewritten to allow for ion/ion reactions between polyanionic peptides and reagent cations. Fluoranthene was chosen as the NETD reagent because it encourages reasonably good fragmentation efficiency while limiting the occurrence of higher energy fragmentation channels that tend to produce chaotic spectra.[18]

LC-MS/MS Analysis. MS^1 spectra were acquired at a resolving power of 60 000 and an automatic gain control (AGC) target value of 1 000 000 charges. Following MS^1 analysis, the ten most intense precursors were selected for data-dependent activation using NETD. Precursors with charge states equal to one or unassigned were rejected, and a 60 s dynamic exclusion window was employed. The MS^2 fragment ion mixture was analyzed using the dual cell linear quadrupole ion trap. Though we initially considered analyzing the MS^2 fragment ions in the orbitrap, quadrupole ion trap analysis was more compatible with the low flux of peptide anions (vide infra) because of its greater sensitivity. MS^2 AGC targets were set to 40 000 for the anion population and 400 000 for the reagent cation. The NETD reaction time was set to 100 ms. AGC target values and NETD reaction times were experimentally determined as the best compromise between product ion generation, product ion signal-to-nose, and MS/MS duty cycle.

The MS^1 conditions remained the same for the positive mode analyses involving ETD and CAD, as did the data-dependent precursor selection parameters. For CAD, the normalized collision energy was set to 35. For ETD, the reaction time was set to 60 ms and the reagent cation AGC target was set to 400 000. In both cases, the MS^2 AGC target was set to 10 000.

Data Analysis. The resulting data files were searched with the Open Mass Spectrometry Search Algorithm (OMSSA) version 2.1.8.[35] Prior to this work, OMSSA was not capable of processing MS/MS spectra containing anionic peptide fragments, and no sequence search algorithms were capable of searching for a$^\bullet$-type product ions. MS/MS spectra were searched against the SGD yeast databases. The database was concatenated with reversed versions of the same database. Prior to the use of the sequence search algorithm, MS/MS spectra were "cleaned"; i.e., the charge reduced product ions as well as neutral-loss fragment ions were removed from the spectra.[36,37] Full trypsin or GluC enzymatic specificity was required, allowing up to 3 missed cleavages. Carbamidomethylation of cysteine was specified as a fixed modification, while oxidation of methionine was specified as a variable modification. An average mass tolerance of ±2.5 Da was used for precursors (in an effort to encompass all possible C12/C13 variants), while a monoisotopic mass tolerance of ±0.25 Da was used for products. Following spectral searching, the resulting peptide spectral matches (PSMs) were filtered to a 1% false discovery rate (FDR) using both e-value and precursor mass accuracy (following monoisotopic peak correction, the precursor mass error range was ±3.2 ppm) as described previously.[38,39] When pooling spectra from multiple LC-MS/MS analyses, the FDR was calculated for the aggregate set of data rather than calculating an FDR for each run separately prior to combining the results.

RESULTS AND DISCUSSION

Using our NETD-based LC-MS/MS workflow, which employs basic LC separations and a NETD compatible version of OMSSA, we identified more than 2000 unique peptides from *Saccharomyces cerevisiae* whole-cell lysates. To collect and process such large data sets of peptide anion NETD MS/MS spectra, we had to develop three interlocking pieces in parallel; i.e., the NETD capable mass spectrometer, the high pH LC separation technique, and the NETD compatible search algorithm all had to be devised, characterized, and stably implemented to realize a robust high-throughput NETD-based peptide anion LC-MS/MS method.

Mass Spectrometry. We modified a quadrupole linear ion trap-orbitrap hybrid mass spectrometer to perform NETD. Our laboratory previously adapted orbitrap-based systems for ETD of positive cationic precursors,[31,32] which demonstrated that combining the fragmentation functionality of ETD with the high-mass accuracy and resolving power of the orbitrap allowed access to previously unattainable sample depths and enabled new methods (e.g., decision-tree driven MS/MS analysis).[2] We modified an ETD-enabled dual cell quadrupole linear ion trap-orbitrap system to generate positive reagent ions for ion/ion reactions with anionic peptide precursors (Figure 2). No hardware modifications were necessary; rather, we devised, implemented, and optimized new anion injection schemes, EI/CI source conditions, etc. Radical fluoranthene reagent cations were formed at the EI/CI source in a CI ion volume and in the presence of nitrogen gas. The reagent cations were then transmitted to the high pressure trap of the dual cell quadrupole linear ion trap using a potential gradient with a net offset of −12 V (relative to the CI source). Automated optimization routines were created to tune the various DC offsets and RF amplitudes of the ion-transfer optics between the high-pressure trap and the EI/CI source. Once injected into the trap, the reagent cations and the precursor anions were reacted via charge-sign independent trapping (i.e., RF voltages were applied to both the rods and lenses of the high-pressure quadrupole ion trap to confine both the anions and cations in the same space at the same time). The ion/ion reaction was quenched by raising the center section of the quadrupole ion trap to 12 V (positive). In this manner, the anionic product ions were retained and the remaining cationic reagents were ejected. Following quenching, the product ions were transferred to the low-pressure quadrupole ion trap for m/z analysis. We had originally planned on analyzing the MS/MS product ion population in the orbitrap; however, because of the low flux of precursor peptide anions we elected to employ the higher sensitivity quadrupole ion trap analyzer. All MS^1 ion populations were analyzed in the orbitrap. Figure 1 displays

an NETD tandem mass spectrum produced using the NETD-enabled instrument. This mass spectrum results from the reaction of radical fluoranthene cations with doubly deprotonated human angiotensin I peptide. From these data we can easily determine the peptide primary sequence from the abundant $a^{\bullet}$- and x-type fragments that provide extensive sequence coverage.

High pH nLC Separations. The transition from infusion experiments to nLC-MS/MS was straightforward from an instrumentation perspective because the pre-existing Velos-Orbitrap nLC-MS/MS acquisition software supported data-dependent interrogation of precursors, regardless of their polarity. As such, no additional instrument modifications were necessary. Note that certain allowances were made when establishing broadly applicable NETD scan parameters; that is, the predominance of doubly charged peptide anions among the negative ESI ion mixture (vide infra) necessitated longer ion/ion reaction times and higher MS/MS AGC targets than are typically used during ETD ion/ion reactions (i.e., 100 ms and 40 000 for NETD vs 60 ms and 10 000 for ETD).

The primary obstacle to implementing NETD nLC-MS/MS experiments was developing a high pH LC separation method in the nanoflow regime. The use of high pH mobile phases presented technical obstacles that challenged chromatographic reproducibility, spray stability, and overall technique robustness. In situ cast silicate-based frits, routinely used in capillary nLC column fabrication, are very durable at low pH[40] but unpredictably dislodged or fractured in as little as 12 h of continuous operation at pH 10. Frit failures resulted in erratic high-pressure spikes and flow fluctuations, consequently resulting in irreproducible chromatography and leaks at finger-tight PEEK fittings. Dislodged precolumn frits bled stationary phase into the tee and eventually displaced the entirety of precolumn stationary phase into the vent/waste line, while pieces of, and at times entire, frits from analytical columns would often be injected into the tip, catastrophically compromising spray stability. The increased failure rate of these frits, which we attributed to rapid dissolution of the silicate-based frit at high pH, was exacerbated by the large surface area of the frit and its bond to another silicate-based material (fused silica). Due to the numerous complications associated with the cast frits, we eliminated them all together, instead, opting for a packed tip analytical column design coupled to precolumns that were slurry-packed while attached to nanotees, housing titanium, or stainless steel frits. This precolumn design provided superior chromatography to end fittings with embedded frits and was sturdier than PEEK sleeves with integrated terminal frits. We tried eliminating the use of a precolumn and opting for direct injection onto the analytical column. However, the sample loading time increased by a factor of 4−5 due to the decreased flow rate leading to a substantial reduction in sample throughput. Moreover, premature analytical column/emitter fouling increased to an unacceptable rate without the use of a precolumn. An additional complication was that the ESI emitter, integrated into the analytical column, would frequently close or become blocked resulting in poor or no spray. Spray problems were alleviated by brief chemical etching of the laser-pulled tip (~1 um diameter) in hydrofluoric acid (vide supra) to produce a larger tip opening (~5 um) and tip geometry that was less prone to clogging and promoted more consistent negative ESI. We tested buffer concentrations from 1 to 20 mM ammonium formate and found 5 mM to be a good compromise when considering buffering capacity, minimization of salt adduction, MS^1 signal-to-noise, and promotion of stable negative ESI.

Database Searching. With thousands of NETD-MS/MS spectra in hand, we encountered another obstacle: no sequence search algorithm was capable of handling $a^{\bullet}$- and x-type product anions. Although a few algorithms were capable of searching for anionic peptide fragments (e.g., b- and y-type anions), the overall dearth of support is indicative of the infancy of this method. We modified the search algorithm OMSSA to support NETD MS/MS spectral analysis[35] and then searched all MS/MS spectra against the SGD yeast database concatenated with reversed versions for establishment of false discovery rates (all data was filtered to a 1% FDR).[39]

As this was the first effort to process large NETD MS/MS data sets using a sequence search algorithm, we made various efforts to optimize sensitivity; e.g., in addition to searching for only $a^{\bullet}$- and x-type fragment ions, we also tested whether searching for CO_2 neutral loss species improved sensitivity. We hypothesized that due to sequential ion/ion reactions and the relatively prevalent CO_2 neutral loss fragment pathway, precursors with charge states greater than two would tend to accrue $a^{\bullet}$- and x-type fragment ions that have a CO_2 neutral loss, in addition to the intact $a^{\bullet}$- and x-type species. We searched our data using every possible combination of $a^{\bullet}$, x, $a^{\bullet}$-CO_2 and x-CO_2 type fragment ions. For each set of search conditions, we calculated the average probability that precursors with a given charge state would result in a high-confidence (1% FDR) peptide spectral match (Figure 3). Though searching for the more complex fragment ion series was slightly beneficial when querying MS/MS spectra of highly charged precursors, very few precursor ions were formed with

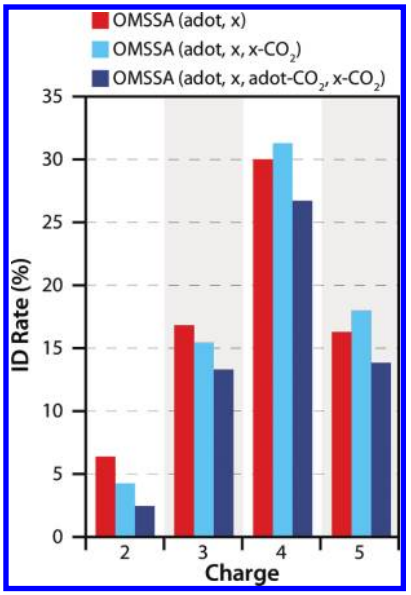

Figure 3. MS/MS spectra produced during the NETD-based nLC-MS/MS analysis of a yeast sample were searched by OMSSA (version 2.1.8) using different fragment ion series. Highly charged precursor ions tend to undergo sequential ion/ion reactions, which often results in multiple bond cleavages. Thus, searching for a complex set of fragment ions that includes $a^{\bullet}$-, x-, $a^{\bullet}$-CO_2 and x-CO_2 type is advantageous when considering highly charged precursors. However, the occurrence of these precursor ions is quite rare under NESI conditions, so it is generally more sensitive and faster to search for the simpler ion series of $a^{\bullet}$- and x-type fragment ions.

dx.doi.org/10.1021/ac203430u | Anal. Chem. 2012, 84, 2875−2882

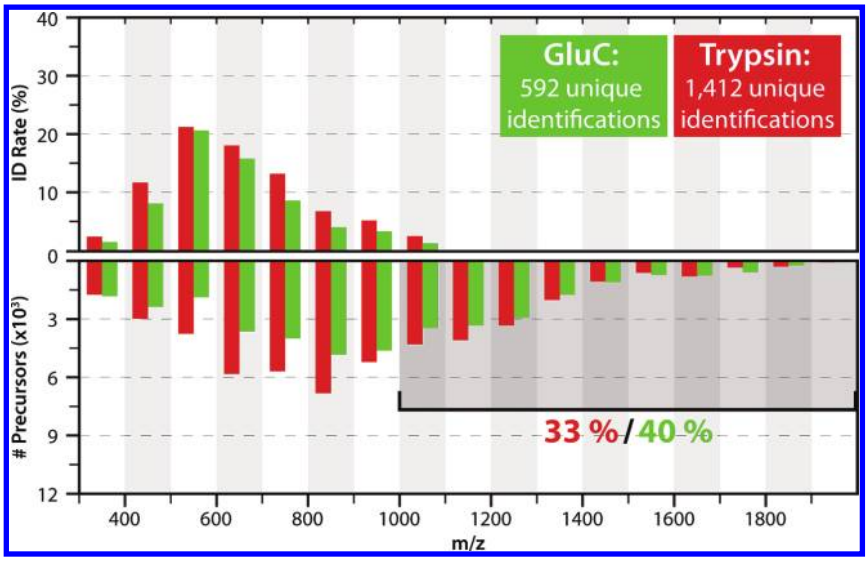

Figure 4. Comparison of the peptides identified using negative ESI nLC-NETD-MS/MS analysis of complex mixtures produced by digesting a yeast whole cell lysate with either GluC or trypsin. The precursor population was sorted by precursor m/z (lower panel), and the success rate for each bin was calculated (upper panel). In general, whether formed using trypsin or GluC, peptides between 400 m/z and 900 m/z are most amenable to NETD-MS/MS. GluC tends to produce larger peptides that are more likely to fall outside this range (40% of all GluC peptides are above 1000 m/z, while 33% of tryptic peptides are about 1000 m/z).

these higher charge states (vide infra); hence, searching for only $a^{\bullet}$- and x-type fragment ions was the most generally applicable search parameters and, therefore, the most likely to produce high scoring peptide spectral matches. Ultimately, an approach that tailors the hypothetical fragment ion series to precursor charge state should allow for the greatest sensitivity and future implementations of the search algorithm will take this into consideration.

Shotgun Sequencing with Negative ESI and NETD MS/MS. Using these newly developed interlocking pieces, an NETD-capable Orbitrap, high pH nLC separations, and a complete data-analysis pipeline, we began testing the performance of shotgun proteomics in the negative ionization mode. We split a yeast whole cell lysate, digested the aliquots with either trypsin or GluC, and analyzed, in triplicate, the resulting complex peptide mixtures by negative ESI-nLC-MS/MS using NETD and a 2 h gradient. We produced 3713 high-quality PSMs and 2004 unique peptide identifications (1412 and 592 unique IDs from trypsin and GluC, respectively) from unfractionated yeast whole-cell lysate.

As a tool to understanding the strengths and limitations of the method, we produced a histogram of the probability of producing a peptide spectral match that was distributed by precursor m/z (Figure 4). As a complement to this histogram, we also plotted the number of precursor ions at each of those m/z values. As is typical of all ion/ion-based fragmentation methods, we had difficultly successfully querying high m/z precursor ions. Initially, we hypothesized that GluC peptides might be more amenable to NETD interrogation than tryptic ions because of the carboxylic acid moieties on both the GluC side-chain and C-terminus. We were hopeful that the prevalent anionic charge sites would promote higher charge densities. However, compared to tryptic peptides ionized by negative ESI, GluC peptides tend to form higher m/z precursors because the peptides tend to be longer (due to a decrease in the frequency of cleavage sites between trypsin and GluC) and there is no concurrent increase in charge state; i.e., of all the GluC peptides interrogated, 40% had m/z values greater than 1000 while only 33% of the tryptic precursors had such high values.

Interestingly, at any given m/z value, an NETD spectra of a GluC peptide has less of a chance of producing a peptide spectral match than a tryptic peptide. We hypothesize that this decrease in the identification rate of GluC peptides may be due to an increase in charge localizing sites (e.g., carboxylic acid moieties) at the C-terminal side of the peptide. By localizing two potential charge bearing sites on the same side of the peptide, we increase the chances of exclusively seeing fragment ions from that end (i.e., following fragmentation, it is more likely that the remaining charge will be exclusively located at the C-terminus). This would result in a more homogeneous population of fragment ions and ultimately would provide fewer data points for the database correlation algorithm. This will be explored more fully in future work that examines the relationships between peptide primary sequence and NETD fragmentation pathways.

Comparisons to Positive Mode LC-MS/MS Workflows. To compare our NETD-based results to conventional positive mode shotgun analyses, we analyzed the same trypsinized yeast sample using the typical low pH shotgun strategy with ETD and CAD MS/MS. Both of these methods produced more unique identifications than the NETD-based analyses, 4403 (ETD) and 6693 (CAD). However, as this is the first attempt to interrogate a very complex sample using an NETD-based LC-MS/MS method, to be within a factor of 3 is a strong initial performance. While each interlocking piece of our NETD-based nLC-MS/MS workflow will no doubt benefit from optimization and further development, the analysis of the peptides we identified using the current NETD-based method reveals strong complementarity with the positive mode results (Supplementary Figure 1, Supporting Information).

Negative ESI, as observed by us as well as by others, produces a substantially lower flux of precursor ions than positive ESI.[41,42] The lower flux is very closely related to spray instability, a frequent concern during our analyses. It is thought that negative ESI can promote corona discharge at, or near, the

dx.doi.org/10.1021/ac203430u | Anal. Chem. 2012, 84, 2875−2882

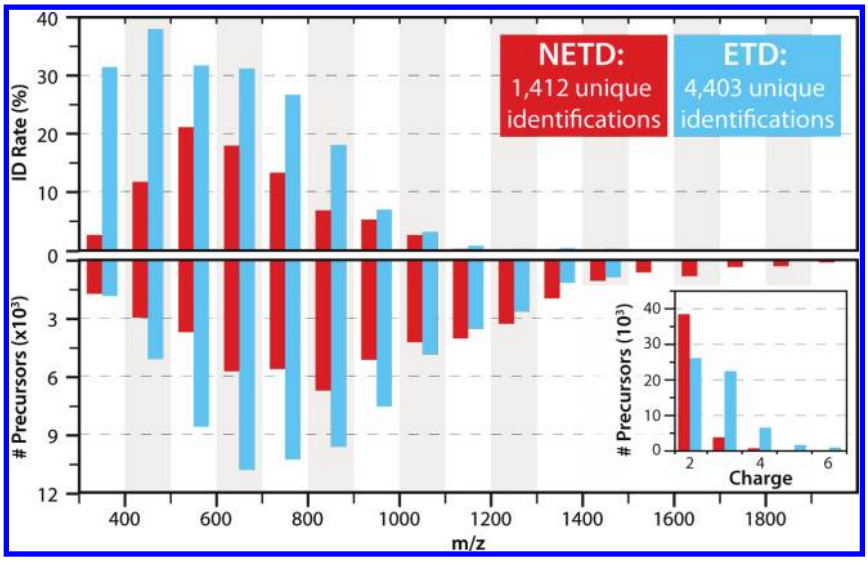

Figure 5. Comparison of the peptides identified by either negative ESI nLC-NETD-MS/MS or positive ESI nLC-ETD-MS/MS analysis of complex mixtures that were formed by digesting a yeast whole cell lysate with trypsin. The precursor population was sorted by precursor m/z (lower panel), and the success rate for each bin was calculated (upper panel). On average, negative ESI produces more lowly charged precursors than positive ESI (inset), which results in a significantly reduce identification rate (upper panel).

ESI emitter orifice. Once corona discharge occurs, the transmission of ions from solution into the gas phase is greatly diminished.[43,44] High electron affinity bath gases (O_2, SF_6) and halogenated solution additives have been used to scavenge electrons to reduce the occurrence of corona discharge; however, these approaches have been neither universally successful nor applicable. The corona discharge phenomenon is especially problematic for the highly conductive, aqueous solutions used for peptide separations.[43] The most immediate impact of this decreased flux is a lengthening of the duty cycle of the NETD-MS/MS scan. With negative ESI, the average injection time of the analytical scans increase 2-fold (117.8 ms vs 50.6 ms for NETD vs ETD), which in turn causes fewer mass spectra to be collected (48 472 vs 67 012) and lowers overall sensitivity. Additionally, negative ESI almost exclusively produced doubly charged precursor ions, whereas positive ESI produced a much more heterogeneous mixture of precursor charge states that included many species with high-charge densities ($z > 2$). This is evident in the lower two histograms of Figure 5, which detail, by m/z and charge state, all the precursors interrogated by the NETD and ETD methods. The predominantly lowly charged mixture of ions produced by negative ESI is less desirable, because NETD, like ETD, performs optimally with precursors of higher charge density. Also, the tendency of negative ESI to produce lowly charged precursors, and the compatibility of NETD with low m/z precursors, compound such that the NETD-based method tends to identify shorter peptides when compared to the positive mode workflows (14.5, 18.4, and 17.3 residues per peptides for NETD, ETD, and CAD, respectively; Table 1).

As expected, the basic mobile phases and negative ESI conditions of the NETD MS/MS method favored acidic peptides, while the acidic mobile phases and positive ESI conditions of the standard shotgun method were biased toward more basic sequences. This conclusion is evinced by the calculated pI values of the peptides identified under negative and positive ESI conditions: 5.0, 5.8, and 5.7 for NETD, ETD, and CAD MS/MS, respectively (Table 1, Tables S4–S6 Supporting Information). This divergence is even more pronounced when considering only peptide identifications that were unique to each of the specific data sets (i.e., excluding any peptide identifications that were shared between NETD MS/MS and the positive ESI methods): 4.8 vs 5.9 (NETD vs ETD) and 5.3 vs 5.8 (NETD vs CAD). The depressed pI values of the peptides unique to the NETD MS/MS analyses were largely due to a decreased occurrence of basic residues in that population: the NETD, ETD, and CAD MS/MS methods identified on average 1.3, 2.0, and 1.9 basic residues per peptide, whereas the average number of acidic residues per peptide remained relatively constant at 2.7, 2.8, and 2.6. A similar divergence was noted between the calculated hydrophobicity factors of the NETD, ETD, and CAD data sets (Supporting Information).

Table 1. Peptide Identifications by Fragmentation Method[a]

	NETD	ETD	CAD
unique IDs	1412	4403	6693
average peptide pI	5.0	5.8	5.7
average peptide hydrophobicity	27.7	31.6	30.9
average number of basic residues (per peptide)	1.3	2.0	1.9
average number of acidic residues (per peptide)	2.7	2.8	2.6
average number of hydrophobic residues (per peptide)	4.6	5.9	5.8
average peptide length (in residues)	14.5	18.4	17.3

[a]A yeast lysate was digested with trypsin, separated over a 2 h gradient, and analyzed using either negative ESI and NETD-MS/MS or positive ESI with both ETD- and CAD-MS/MS (in triplicate). The resulting unique peptide identifications for each method are shown. Though the NETD MS/MS method produced fewer overall identifications, the method identified chemically distinct sequences.

Implications for Proteome Coverage. By accessing lower pI segments of the proteome with negative ESI and NETD MS/MS, we often enhanced observed sequence coverage (Table S1, Supporting Information). Take, for example, the acidic protein GRX1 (pI = 4.8), an important glutaredoxin capable of reducing hydroperoxides and protecting

dx.doi.org/10.1021/ac203430u | Anal. Chem. 2012, 84, 2875–2882

cells against oxidative damage.[45] The positive ESI methods produced 29% (ETD) and 50% (CAD) sequence coverage from tryptic peptide cations, with respective pI averages of 5.6 and 5.4. The negative ESI approach generated 45% sequence coverage from tryptic peptide anions, with an average pI of 4.5, which permitted observation of the last 27 residues of the highly acidic c-terminus (Figure 6). NETD MS/MS, in

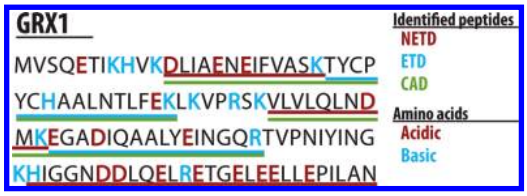

Figure 6. By accessing lower pI segments of the proteome with negative ESI and NETD MS/MS, NETD enhances coverage for acidic proteins like GRX1 (pI = 4.8), an important glutaredoxin capable of reducing hydroperoxides and protecting cells against oxidative damage.[45] The negative ESI approach generated 45% sequence coverage from tryptic peptide anions, with an average pI of 4.5, and permitted observation of the last 27 residues of the highly acidic c-terminus.

combination with ETD or CAD MS/MS, increased the sequence coverage of the GRX1 protein to 75% (Table S2, Supporting Information).

Even when applied to highly basic proteins, NETD improves sequence coverage by successfully interrogating the more acidic regions of their primary sequences. Consider the high pI values of ribosomes: the majority of proteins from the 40S and 60S ribosomal subunits have pI values greater than 11. The high pI may reflect electrostatic interactions involved in the binding of negatively charged nucleic acids.[46] By only sequencing predominantly basic peptides, the positive ESI shotgun approach generated only modest sequence coverage for many ribosomal proteins. The negative ESI NETD MS/MS method, on the other hand, boosted sequence coverage by permitting access to the acidic portions of these proteins (Table S3, Supporting Information). For example, the 60S ribosomal subunit protein RPL6B has a pI of 10.9. Positive ESI with either ETD or CAD MS/MS only achieved 26% and 27% sequence coverage because the methods were biased toward peptides with high pI values (8.2 and 7.1, respectively). However, negative ESI, along with NETD MS/MS, covered 33% of the sequence of RPL6B, more than either of the positive mode methods, by successfully interrogating peptides with an average pI of 6.2.

CONCLUSIONS

NETD tandem MS presents a direct route to sequencing peptide anions on a rapid, chromatography compatible time-scale. Coupled with robust nLC methods that utilize basic mobile phases, negative ESI, and an NETD compatible version of OMSSA, large-scale shotgun analysis of the yeast proteome using NETD MS/MS produced several thousand high quality PSMs. This is many fold more peptide anion identifications than has previously been produced using any other negative ion fragmentation technique.

However, when analyzed in the positive mode (i.e., low pH LC conditions, positive ESI, and either CAD or ETD), the same sample resulted in ~3 times the number of PSMs. The principle hurdle to making the NETD-based method as generally applicable to complex peptide mixtures as the positive mode analogs is the flux of and mixture of ions produced by the negative ESI source. Negative ESI, as observed by us as well as by others, produces a substantially lower flux of precursor ions than positive ESI.[41,42] Future advancements in the negative ESI NETD-MS/MS method described here will likely come from improving negative ESI performance, via alterations to mobile phase pH, for example, or as an alternative to increasing the distribution of precursor charge states, NETD can be partnered with concurrent or supplemental activation (i.e., NETcaD or AI-NETD).[47−49] These techniques would help obviate the low m/z bias of the NETD technique and would consequently improve the compatibility of the fragmentation method with the lowly charged precursor distribution produced by negative ESI.

In spite of its reduced sensitivity, performing shotgun protein analysis using the NETD-based nLC-MS/MS workflow presented here permits the identification of acidic and previously unseen segments of the proteome. This utility is evidenced by the tendency to identify peptides with lower pI values using NETD than either of the positive mode analogs. This trend toward identifying low pI peptides results in improved sequence coverage with NETD than either ETD or CAD is capable of alone; e.g., with NETD, we can directly observe the acidic termini of GRX1 which is overlooked by the positive-mode methods. This proof of concept compatibility with the acidic segments of the proteome encourages the application of this technology to other biologically interesting samples that are incompatible with the traditional positive-mode workflows; e.g., the analysis of histidine phosphopeptides is uniquely compatible with an NETD-centric workflow because that modification is rapidly lost when placed in solutions of pH < 6.[5−9]

ASSOCIATED CONTENT

Supporting Information

Additional information as noted in text. This material is available free of charge via the Internet at http://pubs.acs.org.

AUTHOR INFORMATION

Corresponding Author

*Tel.: + 1 608 263 1718. Fax: 1 608 890 0167. E-mail: jcoon@chem.wisc.edu.

Notes

The authors declare no competing financial interest.

ACKNOWLEDGMENTS

G.C.M. and J.D.R. contributed equally to this work. We thank AJ Bureta for figure design, Craig D. Wenger and Derek J. Bailey for assistance with data analysis, Jae C. Schwartz for helpful discussions, and Sarah Jacob for aid in manuscript preparation. We are grateful to Thermo Fisher Scientific and the National Institutes of Health (R01GM080148 to J.J.C.) for providing funding for this work. This research was supported in part by the Intramural Research Program of the NIH, National Library of Medicine.

REFERENCES

(1) de Godoy, L. M. F.; Olsen, J. V.; Cox, J.; Nielsen, M. L.; Hubner, N. C.; Frohlich, F.; Walther, T. C.; Mann, M. *Nature* **2008**, *455*, 1251−U1260.

(2) Swaney, D. L.; McAlister, G. C.; Coon, J. J. *Nat. Meth.* **2008**, *5*, 959−964.

(3) Swaney, D. L.; Wenger, C. D.; Coon, J. J. *J. Proteome Res.* **2010**, *9*, 1323−1329.
(4) Washburn, M. P.; Wolters, D.; Yates, J. R. *Nat. Biotechnol.* **2001**, *19*, 242−247.
(5) Hultquist, D. E. *Biochim. Biophys. Acta, Bioenerg.* **1968**, *153*, 329−340.
(6) Wei, Y.-F.; Matthews, H. R. In *Methods in Enzymology*; Tony Hunter, B. M. S., Ed.; Academic Press, San Diego, CA, 1991; Vol. *200*, p 388−414.
(7) Matthews, H. R. *Pharmacol. Ther.* **1995**, *67*, 323−350.
(8) Lasker, M.; Bui, C. D.; Besant, P. G.; Sugawara, K.; Thai, P.; Medzihradszky, G.; Turck, C. W. *Protein Sci.* **1999**, *8*, 2177−2185.
(9) Sickmann, A.; Meyer, H. E. *Proteomics* **2001**, *1*, 200−206.
(10) Bowie, J. H.; Brinkworth, C. S.; Dua, S. *Mass Spectrom. Rev.* **2002**, *21*, 87−107.
(11) Brinkworth, C. S.; Dua, S.; McAnoy, A. M.; Bowie, J. H. *Rapid Commun. Mass Spectrom.* **2001**, *15*, 1965−1973.
(12) Steinborner, S. T.; Bowie, J. H. *Rapid Commun. Mass Spectrom.* **1996**, *10*, 1243−1247.
(13) Steinborner, S. T.; Bowie, J. H. *Rapid Commun. Mass Spectrom.* **1997**, *11*, 253−258.
(14) Anusiewicz, I.; Jasionowski, M.; Skurski, P.; Simons, J. *J. Phys. Chem. A* **2005**, *109*, 11332−11337.
(15) Budnik, B. A.; Haselmann, K. F.; Zubarev, R. A. *Chem. Phys. Lett.* **2001**, *342*, 299−302.
(16) Coon, J. J.; Shabanowitz, J.; Hunt, D. F.; Syka, J. E. P. *J. Am. Soc. Mass Spectrom.* **2005**, *16*, 880−882.
(17) Crizer, D. M.; Xia, Y.; McLuckey, S. A. *J. Am. Soc. Mass Spectrom.* **2009**, *20*, 1718−1722.
(18) Huzarska, M.; Ugalde, I.; Kaplan, D. A.; Hartmer, R.; Easterling, M. L.; Polfer, N. C. *Anal. Chem.* **2010**, *82*, 2873−2878.
(19) Kjeldsen, F.; Silivra, O. A.; Ivonin, I. A.; Haselmann, K. F.; Gorshkov, M.; Zubarev, R. A. *Chem.—Eur. J.* **2005**, *11*, 1803−1812.
(20) Larraillet, V.; Vorobyev, A.; Brunet, C.; Lemoine, J.; Tsybin, Y. O.; Antoine, R.; Dugourd, P. *J. Am. Soc. Mass Spectrom.* **2010**, *21*, 670−680.
(21) Ganisl, B.; Valovka, T.; Hartl, M.; Taucher, M.; Bister, K.; Breuker, K. *Chem.—Eur. J.* **2011**, *17*, 4460−4469.
(22) Antoine, R.; Joly, L.; Tabarin, T.; Broyer, M.; Dugourd, P.; Lemoine, J. *Rapid Commun. Mass Spectrom.* **2007**, *21*, 265−268.
(23) Madsen, J. A. M. J. A.; Kaoud, T. S.; Dalby, K. N.; Brodbelt, J. S. *Proteomics* **2011**, *11*, 1329−1334.
(24) Wolff, J. J.; Leach, F. E.; Laremore, T. N.; Kaplan, D. A.; Easterling, M. L.; Linhardt, R. J.; Amster, I. J. *Anal. Chem.* **2010**, *82*, 3460−3466.
(25) Leach, F. E.; Wolff, J. J.; Xiao, Z. P.; Ly, M.; Laremore, T. N.; Arungundram, S.; Al-Mafraji, K.; Venot, A.; Boons, G. J.; Linhardt, R. J.; Amster, I. J. *Eur. J. Mass Spectrom.* **2011**, *17*, 167−176.
(26) Barlow, C. K.; Hodges, B. D. M.; Xia, Y.; O'Hair, R. A. J.; McLuckey, S. A. *J. Am. Soc. Mass Spectrom.* **2008**, *19*, 281−293.
(27) Huang, T. Y.; McLuckey, S. A. *Int. J. Mass Spectrom.* **2011**, *304*, 140−147.
(28) Kjeldsen, F.; Horning, O. B.; Jensen, S. S.; Giessing, A. M. B.; Jensen, O. N. *J. Am. Soc. Mass Spectrom.* **2008**, *19*, 1156−1162.
(29) Yang, J.; Hakansson, K. *Int. J. Mass Spectrom.* **2008**, *276*, 144−148.
(30) Valaskovic, G. A.; Kelleher, N. L.; Little, D. P.; Aaserud, D. J.; McLafferty, F. W. *Anal. Chem.* **1995**, *67*, 3802−3805.
(31) McAlister, G. C.; Berggren, W. T.; Griep-Raming, J.; Horning, S.; Makarov, A.; Phanstiel, D.; Stafford, G.; Swaney, D. L.; Syka, J. E. P.; Zabrouskov, V.; Coon, J. J. *J. Proteome Res.* **2008**, *7*, 3127−3136.
(32) McAlister, G. C.; Phanstiel, D.; Good, D. M.; Berggren, W. T.; Coon, J. J. *Anal. Chem.* **2007**, *79*, 3525−3534.
(33) McAlister, G. C.; Phanstiel, D.; Wenger, C. D.; Lee, M. V.; Coon, J. J. *Anal. Chem.* **2010**, *82*, 316−322.
(34) Olsen, J. V.; Schwartz, J. C.; Griep-Raming, J.; Nielsen, M. L.; Damoc, E.; Denisov, E.; Lange, O.; Remes, P.; Taylor, D.; Splendore, M.; Wouters, E. R.; Senko, M.; Makarov, A.; Mann, M.; Horning, S. *Mol. Cell. Proteomics* **2009**, *8*, 2759−2769.
(35) Geer, L. Y.; Markey, S. P.; Kowalak, J. A.; Wagner, L.; Xu, M.; Maynard, D. M.; Yang, X. Y.; Shi, W. Y.; Bryant, S. H. *J. Proteome Res.* **2004**, *3*, 958−964.
(36) Good, D.; Wenger, C.; McAlister, G.; Bai, D.; Hunt, D.; Coon, J. *J. Am. Soc. Mass Spectrom.* **2009**, *20*, 1435−1440.
(37) Good, D. M.; Wenger, C. D.; Coon, J. J. *Proteomics* **2010**, *10*, 164−167.
(38) Wenger, C. D.; Phanstiel, D. H.; Lee, M. V.; Bailey, D. J.; Coon, J. J. *Proteomics* **2011**, *11*, 1064−1074.
(39) Elias, J. E.; Gygi, S. P. *Nat. Meth.* **2007**, *4*, 207−214.
(40) Ficarro, S. B.; Zhang, Y.; Lu, Y.; Moghimi, A. R.; Askenazi, M.; Hyatt, E.; Smith, E. D.; Boyer, L.; Schlaeger, T. M.; Luckey, C. J.; Marto, J. A. *Anal. Chem.* **2009**, *81*, 3440−3447.
(41) Cech, N. B.; Enke, C. G. *Mass Spectrom. Rev.* **2001**, *20*, 362−387.
(42) Yamashita, M.; Fenn, J. B. *J. Phys. Chem.* **1984**, *88*, 4671−4675.
(43) Hiraoka, K.; Kudaka, I. *Rapid Commun. Mass Spectrom.* **1992**, *6*, 265−268.
(44) Straub, R. F.; Voyksner, R. D. *J. Am. Soc. Mass Spectrom.* **1993**, *4*, 578−587.
(45) Collinson, E. J.; Wheeler, G. L.; Garrido, E. O.; Avery, A. M.; Avery, S. V.; Grant, C. M. *J. Biol. Chem.* **2002**, *277*, 16712−16717.
(46) Shazman, S.; Mandel-Gutfreund, Y. *PLoS Comput. Biol.* **2008**, *4*, e1000146.
(47) Ledvina, A. R.; Beauchene, N. A.; McAlister, G. C.; Syka, J. E. P.; Schwartz, J. C.; Griep-Raming, J.; Westphall, M. S.; Coon, J. J. *Anal. Chem.* **2010**, *82*, 10068−10074.
(48) Ledvina, A. R.; McAlister, G. C.; Gardner, M. W.; Smith, S. I.; Madsen, J. A.; Schwartz, J. C.; Stafford, G. C.; Syka, J. E. P.; Brodbelt, J. S.; Coon, J. J. *Angew. Chem., Int. Ed.* **2009**, *48*, 8526−8528.
(49) Swaney, D. L.; McAlister, G. C.; Wirtala, M.; Schwartz, J. C.; Syka, J. E. P.; Coon, J. J. *Anal. Chem.* **2007**, *79*, 477−485.